



Studies on synthesis and physiochemical evaluation of curcumin-loaded chitosan nanoparticles

Eltobgy Ahmed Magdy¹, Gamal Osman Elhassan², Syeda Ayesha Farhana², Riyaz Ahmed Khan², Siham A. Abdoun², R. A. M. Jainaf Nachiya³, Jamal Moideen Muthu Mohamed^{1*}

¹Faculty of Pharmacy & BioMedical Sciences, MAHSA University, Jenjarom, Malaysia.

²Department of Pharmaceutics, College of Pharmacy, Qassim University, Buriadah, Saudi Arabia.

³Crescent School of Pharmacy, BS Abdur Rahman Crescent Institute of Science and Technology, Vandalur, India.

ARTICLE HISTORY

Received on: 13/02/2025

Accepted on: 10/05/2025

Available Online: 05/07/2025

Key words:

Drug delivery, chitosan, polymeric nanoparticles, top-down method, *in vitro* study.

ABSTRACT

This study aimed to develop curcumin (CMN)-loaded chitosan nanoparticles (C-NPs) as a potential drug delivery system. Unique to this research was the use of a top-down method that allows for precise control over nanoparticle size, which is critical for enhancing stability, efficacy, bioavailability, and controlled drug delivery. The study employed advanced characterization techniques, including Fourier-transform infrared spectroscopy (FTIR), to confirm the successful formation of C-NPs, along with an evaluation of drug loading capacity (LC) and percentage drug entrapment (PDE). Typically, *in vitro* drug release studies were conducted to evaluate the sustained release behavior of C-NPs. The results demonstrated the successful formation of C-NPs with desirable characteristics, with a high LC (86.81% ± 5.44%) and PDE (68.12% ± 4.24%), indicating efficient encapsulation of CMN, which was significantly higher compared to many existing formulations. The sustained release mechanism not only improves bioavailability and efficacy but also facilitates targeted and combination therapies, achieving a release rate of 88.24% ± 6.89% over 24 hours. Moreover, a short-term stability study conducted has proved that the prepared C-NPs might be stable up to 15 days, highlighting their practical applicability. Overall, this study provides valuable insights into the innovative development and characterization of C-NPs as a promising carrier for CMN delivery, offering significant advancements in drug delivery systems that could lead to improved therapeutic strategies.

INTRODUCTION

Nanoparticles (NPs) are ultrafine particles with dimensions in the nanometer range (1100 nm). Their unique properties such as high surface area, small size, and the ability to be engineered for specific functions make them promising tools for medical applications, particularly in the treatment and diagnosis of diseases [1]. NPs can be designed to deliver drugs directly to tumor cells, minimizing side effects on healthy tissues. Metallic NPs can absorb light and convert it to heat,

selectively killing cancer cells. NPs can assist in delivering anti-inflammatory drugs to treat atherosclerosis.

They improve the contrast in imaging techniques, aiding in early diagnosis. Silver and copper NPs show significant antimicrobial properties, useful in treating bacterial infections. NPs can enhance the efficacy of vaccines by improving the immune response [2]. NPs can cross the blood-brain barrier, allowing for targeted therapies in conditions like Alzheimer's and Parkinson's disease. Improved drug solubility and bioavailability and lowered systemic side effects due to targeted therapy. It can be engineered for various functions, making them suitable for multiple applications. Moreover, used for tracking disease progression through imaging. NPs hold significant promise for the treatment of various diseases due to their unique properties and versatility [3]. Ongoing research and technological advancements will likely lead to innovative

*Corresponding Author

Jamal Moideen Muthu Mohamed, Faculty of Pharmacy & BioMedical Sciences, MAHSA University, Jenjarom, Malaysia.

E-mail: jamalmoideen@mahsa.edu.my

applications, improving patient outcomes and redefining disease management approaches.

Curcumin (CMN) is a bioactive compound derived from the turmeric plant (*Curcuma longa*). Known for its vibrant yellow color, it has been used for centuries in traditional medicine, particularly in Ayurvedic and Chinese practices. CMN is recognized for its anti-inflammatory, antioxidant, and potential therapeutic properties [4]. CMN inhibits various inflammatory pathways and cytokines, making it effective in reducing inflammation associated with conditions like arthritis and inflammatory bowel diseases.

CMN has been studied for its potential therapeutic use in a range of diseases, including cancer, cardiovascular conditions, neurodegenerative disorders, diabetes, and inflammatory diseases such as rheumatoid arthritis. It is available as a dietary supplement and is also being evaluated in clinical trials to assess its efficacy and safety in different patient populations [5]. CMN is a promising therapeutic agent with a wide range of potential applications in treating various diseases. Continued research into its mechanisms and efficacy will help unlock its full potential for improving health and combating diseases. While it holds significant promise, further clinical studies are needed to establish optimal dosages and treatment protocols.

CMN produces significant attention in past decades for its potential therapeutic properties, including anticancer antioxidant, and anti-inflammatory effects. However, its therapeutic claim had been hindered primarily by its poor bioavailability. CMN is poorly aqueous soluble, which limits its absorption in the gastrointestinal tract (GIT). After absorption, CMN is readily metabolized and eliminated by the liver, resulting in low systemic availability [6]. Also, the structure molecular structure of CMN affects its ability to permeate cell membranes, further reducing its effectiveness. These issues significantly influence the efficacy of CMN, necessitating design formulation strategies to enhance its delivery and absorption.

Chitosan, a deacetylated derivative of chitin, has emerged as a promising biopolymer for nanoparticle-based drug delivery systems. Its unique properties, including biocompatibility, biodegradability, and cationic charge, make it an attractive candidate for various biomedical applications. Chitosan exhibits excellent biocompatibility with human tissues, reducing the risk of adverse immune responses [7]. It is biodegradable, ensuring safe elimination from the body after drug delivery. The cationic nature of chitosan allows for electrostatic interactions with negatively charged drug molecules, facilitating encapsulation and controlled release. Chitosan can be modified to respond to specific stimuli, such as pH or temperature, enabling targeted drug delivery to specific tissues or cells. Chitosan can improve the solubility of poorly water-soluble drugs, enhancing their bioavailability [8].

Chitosan could improve the solubility of CMN due to its hydrophilic nature by increased solubility facilitates better absorption in the GIT. Chitosan NPs could be engineered to provide a controlled release of CMN which helps to maintain therapeutic levels over an extended period, reducing the need for frequent dosing. Also, chitosan can enhance the targeting NPs to specific tissues or cells by improving the efficacy of CMN, especially in cancer therapy [9].

The biocompatibility of chitosan reduces adverse reactions, making it a suitable candidate for drug delivery applications. This property reduces the risk of long-term accumulation and toxicity and it exhibits inherent antimicrobial activity and is principally beneficial in tissue engineering and wound healing applications [10]. Chitosan can successfully load a wide range of therapeutic agents, especially proteins and peptides, hydrophilic and hydrophobic drugs. Its adaptability improves its suitability for a range of therapeutic methods and permits the administration of various types of drugs. Chitosan has good mucoadhesive properties, allowing it to cling to mucosal surfaces (e.g., nasal cavity, GIT, and so on). This adhesion increases the overall bioavailability, absorption, and extends the residence time at the site of action [11].

Controlled release systems allow for a gradual and sustained release of CMN over an extended period, which helps to maintain therapeutic drug levels in the bloodstream, optimizing its anti-inflammatory, antioxidant, and anticancer effects. Modifying the surface properties of chitosan nanoparticles could achieve targeted delivery to specific tissues or organs of tumors [12]. This localized delivery enhances the therapeutic efficacy of CMN while minimizing systemic availability.

Targeted delivery of CMN can exert its effects directly where needed, such as in cancerous tissues, while limiting exposure to healthy tissues and this selective action minimizes potential side effects, making treatments safer. Sustained release formulations could extend the duration of action of CMN, allowing for less frequent dosing. This convenience can significantly improve patient adherence to treatment regimens [13]. By providing a steady state release of CMN, patients may experience more consistent relief of symptoms, leading to improved quality of life and further inspiring adherence to treatment.

Despite these challenges, ongoing research is focused on addressing these limitations and further exploring the potential of chitosan for nanoparticle-based drug delivery. By optimizing chitosan formulations and exploring novel delivery strategies, researchers aim to create more effective and safe therapeutic approaches. Chitosan is a versatile and promising material for nanoparticle drug delivery systems [8]. Its favorable properties enhance the efficacy and safety of therapeutics, making it a valuable tool in modern medicine. Ongoing research will further explore its potential, leading to innovative drug delivery solutions.

This study will systematically optimize the formulation parameters of curcumin-loaded chitosan nanoparticles (C-NPs), focusing on enhancing CMN encapsulation efficiency and controlled release profiles. Also, the current study employs a comprehensive range of characterization techniques to assess the physical and chemical properties of C-NPs, providing a more detailed understanding of their behavior and efficacy [14,15]. The long-term stability assessments under various environmental conditions, contributing valuable data on the shelf-life and practical applicability of C-NPs and explore the mechanisms of CMN release from C-NPs, focusing on how environmental factors influence release kinetics, thereby filling a critical knowledge gap [16].

MATERIALS AND METHODS

The CMN supply was acquired from SRL Pvt. Ltd. located in Mumbai, India. Chitosan was purchased from S.D. Fine Chem. Pvt. Ltd, Mumbai, India. Sodium deoxycholate and glycerine from Hi Media in Mumbai, India. This study made use of internally produced double distilled water, analytical grade chemicals, and reagents.

Compatibility study

To evaluate a potential interaction (difference in structure) between the drug and excipients, Fourier-transform infrared spectroscopy (FT-IR) analysis was conducted [17]. In an FT-IR spectrophotometer (JASCO/FT-IR-6300, Japan), the IR spectra of the solid samples were examined in the solid powder using the KBr disc method in the wavenumber range of 4,000–400 cm^{-1} at a scan speed of 1 cm^{-1} .

Preparation of C-NPs

Dissolve 200 mg of chitosan in 1% acetic acid to obtain a solution with a concentration of 20 mg/ml and stirred the solution until fully dissolved. Dissolve 100 mg of CMN in 1 ml of ethanol (90%) to achieve a concentration of 10 mg/ml. Add this solution to the chitosan solution while stirring for 10 min at 650 RPM continuously to ensure thorough mixing. Prepare 150 mg of sodium deoxycholate solution (15 mg/ml) separately (Fig. 1). Slowly add the sodium deoxycholate solution dropwise to the chitosan-curcumin mixture while stirring vigorously [18]. Sonics & Materials VCX 750, Inc., Newtown, USA was used to sonicate the solution for 15 minutes (Amplitude 45%; pulse rate 9/3seconds) at 25°C. Pour the C-NP solution into a petri-dish, cover with aluminum foil, poke holes in it, and freeze dried (Christ, Alpha1-2 LD plus, Germany) overnight for 48 hours at -40°C. The freeze-dried powder was collected and used for further analysis. Blank nanoparticles were prepared with the similar described procedure without the drug, CMN.

Construction of calibration curve

CMN content was calculated through the use of UV Spectrophotometric methodology. CMN was dissolved in a small quantity of ethanol (0.1 ml) and the required volume was added to produce a stock solution with 1 mg/ml of CMN. For the preparation stock solution up to 9 $\mu\text{g}/\text{ml}$ concentration, distilled water was used for further dilution. To measure λ_{max} in the 200–800 nm region, aliquots of these solutions were placed into a quartz cell and exposed to a UV spectrophotometer (Agilent Cary 60 UV-Vis Spectrophotometer, USA.) at the wavelength of 425 nm. Double distilled water was used as a

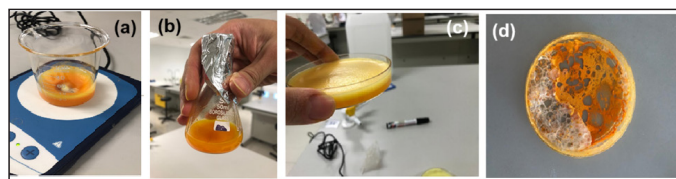


Figure 1. Various stages for the preparation of C-NPs. (a) stirring the solution, (b) prepared C-NPs, (c) petri-dish containing C-NPs for freeze-drying, and (d) freeze-dried solid C-NPs.

blank. The standard calibration curve was created by plotting concentration versus absorbance, and several concentrations of CMN solution were created within the 1–9 $\mu\text{g}/\text{ml}$ range [19]. The selected concentration range should ideally fall within the linear response of the detection by UV-Vis spectroscopy method to ensure the concentrations are in this range helps in obtaining a reliable calibration curve, which is critical for quantitative analysis particularly important in drug delivery systems where effective doses can be low.

Percentage drug entrapment (PDE (%))

The supernatant collected during the NP formulation was used to calculate the PDE (%) of CMN in C-NPs [20]. After centrifugation for 15 minutes at 6,000 rpm, the clear supernatant was collected, and UV-visible spectroscopy was used to analyze it at 425 nm. The drug percentage %EE was computed using equation (3).

$$\% EE (\%) = \frac{\text{A quantity of CMN in C-NPs}}{\text{Total amount of CMN Used}} \times 100 \quad (3)$$

Percentage loading capacity (LC)

Once the freeze-dried C-NPs were dissolved in 0.5 ml of ethanol and the required amount of distilled water for dilution, were filtered through a 0.45 μm membrane filter. A UV-Vis spectrophotometer was then used to detect the concentration of the solution at 425 nm [20]. The following formula was utilized to calculate the DL capacity of C-NPs.

$$LC (\%) = \frac{\text{Quantity of CMN in C-NPs}}{\text{Quantity of C-NPs Obtained}} \times 100 \quad (2)$$

Assay and product yield

The free CMN, NPs, and C-NPs (equal to CMN weight) were sonicated (for 10 minutes with 90 rpm stirring speed) after a 0.5 ml ethanol dilution. UV absorbance was measured and additional dilutions were made using distilled water. The drug content was measured using a standard calibration curve at a wavelength of 425 nm, and the material balance was calculated concerning that content [21]. The yield % concerning the initial amount was calculated using the following formula.

$$\text{Product Yield (\%)} = \frac{\text{Total weight of the C-NPs}}{\text{Total weight of ingredients}} \times 100$$

In vitro drug release

An activated dialysis membrane bag (dialysis membrane 110 (LA 395); molecular weight cutoff of 12,000); Hi-media, Mumbai, India) was used to release CMN from NPs *in vitro* drug release study. It was filled with 1 ml of C-NPs, hermetically sealed, and submerged in 100 ml of phosphate buffer pH 6.8 and release medium at 37°C \pm 1°C while being stirred magnetically (650 rpm) [22]. To keep the sink condition for up to 24 hours, 5 ml of the aliquot was withdrawn at prearranged intervals (1, 2, 3, 6, 8, 12, and 24 hours) and replaced with a new medium (fresh buffer pH 6.8). Following appropriate dilutions, spectrophotometric measurements

were made of the CMN concentration in the samples, and the cumulative percentages of CMN released from the NPs were computed and shown against time.

Release kinetics

To provide a more comprehensive understanding of the drug release mechanism, Higuchi, Hixson Crowell, Korsmeyer Pappas, and release exponent (n) equation models were utilized to calculate the dissolution release kinetics of the NP formulations using both first-order and zero-order calculations [23]. To determine the pattern of release from the SLN, the regression coefficient factor (R^2) and other parameters were computed.

Stability study

To conduct a short-term stability study of the prepared C-NP, Mohamed *et al.* [21] described the method. Briefly, the changes in PDE (%), DC (%), and *in vitro* drug release at room temperature ($25^\circ\text{C} \pm 2^\circ\text{C}$) for 15 days were determined [21].

Statistical analysis

The obtained data are displayed as the mean value and the standard deviation based on three measurements that were taken in triplicate. Following one-way analysis of variance for the statistical analysis of the data using PRISM version 2022 software, the student's *t*-test was employed.

RESULTS AND DISCUSSION

FTIR outcome

Figure 2 displays the FT-IR spectra of Free CMN, sodium deoxy cholate, chitosan, and C-NPs that were used to prepare the C-NPs. The wavenumbers for each spectrum and the characteristics of the functional bands observed. Two peaks in the CMN spectra, at 3322.14 and 3020.22 cm^{-1} , corresponding to $-\text{OH}$ (alcohol) stretch vibrations, were present, suggesting the existence of two hydroxyl groups. It was evident from the peaks at 1739.88 and 1631.29 cm^{-1} that the structure contained $\text{C}=\text{O}$ (carbonyl) groups. According to the earlier investigation published by Mohamed *et al.* [21] the $\text{C}-\text{H}$ (alkane) stretch vibrations at 2931.01 and 2851.09 cm^{-1} and the $\text{C}=\text{C}$ (aromatic) stretch vibrations at 15889.87 and 1510.23 cm^{-1} were also noticeable [21].

Sodium deoxycholate FT-IR spectra (Fig. 2a) revealed a broad band in the $3410\text{--}3188\text{ cm}^{-1}$ range, associated with stretching the $\text{O}-\text{H}$ bond. Furthermore, the carboxylate ester group assignable $-\text{C}=\text{O}$ group in sodium deoxycholate had a strong peak at 1561 cm^{-1} . The stretched $\text{C}-\text{H}$ bond is responsible for the peaks at 2929 and 2871 cm^{-1} . At 1042 cm^{-1} , a second, distinct peak emerged, which was attributed to CCO bonds [24].

The peaks of the CCO bonds in sodium deoxycholate and the $-\text{C}=\text{O}$ group of the carboxylate ester group were completely decreased, as seen in Figure 2b. This is explained by the COO^- group in sodium deoxycholate's involvement in the complexation with the skeleton of polymer structure. Furthermore, the stretching $\text{C}=\text{O}$ originating from each chitosan is displaced, with respective locations of 1734 and 1678 cm^{-1} . The intensity of $\text{N}-\text{H}$ and $\text{O}-\text{H}$ peaks from chitosan

altered due to interactions with CMN, indicating hydrogen bonding. Aromatic $\text{C}=\text{C}$ stretching vibrations from CMN were typically seen between $1508.28\text{--}1598.71\text{ cm}^{-1}$ indicates the CMN successfully incorporated, moreover, shifts in the $\text{C}=\text{O}$ peak position observed, indicating interaction with chitosan [25]. A similar result was reported by Kumbhar *et al.* [26] and they demonstrate that these groups play a significant role in the complexation of the sodium deoxycholate molecule with its functional groups [26].

Determination of λ_{max}

The λ_{max} of CMN was determined first by scanning the solution of CMN in a UV spectrophotometer and the λ_{max} was found to be 425 nm as shown in Figure 3a.

LC (%) and PDE (%)

Although the C-NPs showed an optimal LC ($>80\%$), additional parameters such as reaction time, temperature, or the ratio of the drug to Na precursor may need to be further improved. PDE (%) and LC (%) percentages of C-NPs ranged from $68.12\% \pm 4.24\%$ and $86.81\% \pm 5.44\%$, respectively (Table 1). Chitosan has a positive charge at physiological pH, which enhances its interaction with negative and neutral charged drugs. This electrostatic attraction can significantly increase the amount of drug that can be loaded onto the NP. Also, the porous nature of chitosan NPs allows for the accommodation of a larger volume of both hydrophilic and hydrophobic drugs [10]. At 425 nm ($p > 0.05$), the highest absorption of C-NPs was observed between 200 and 400 nm , accounting for about 80% of the total output sustained. This measurement falls within the reference (label amount) range of 95% to 105% of CMN. Because of its smallest size and highest formulation for LC ($86.81\% \pm 5.44\%$) and PDE ($68.12\% \pm 4.24\%$) in this study. The results showed that the ratio of CMN to chitosan in C-NP was $1:2$ and that CMN had a lipophilic property ($\log p =$

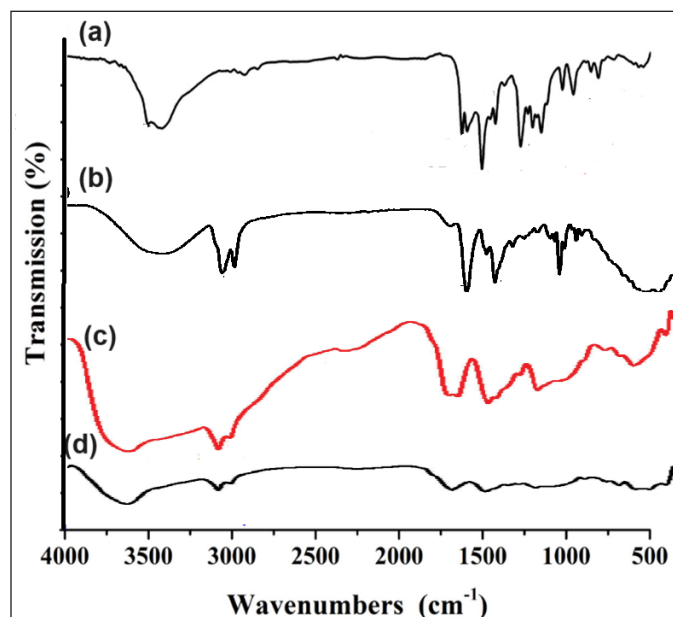


Figure 2. FTIR spectrum of (a) Free CMN, (b) sodium deoxycholate, (c) chitosan, and (d) C-NPs.

3.29). This implies that adding a positively charged carrier, like Na⁺, would improve PDE. By optimizing the CMN-to-chitosan ratio and leveraging the lipophilic nature of CMN along with ionic interactions, the overall PDE of the C-NPs might be improved [10].

Drug content and yield

The quantity (content) of CMN present in the prepared C-NPs varies from 91.27% ± 3.34 % and the material loss concerning the CMN content was calculated to be 3.71% ± 0.44 % of the material (Table 1). According to a previous study [21], lower material loss was seen with C-NPs after the product was obtained. This was caused by an increase in the concentration of chitosan concentration.

The presence of Na⁺ can contribute to the stability of NP by reducing aggregation through electrostatic repulsion. A higher concentration of chitosan typically leads to increased viscosity of the solution, which can improve the encapsulation of CMN within the NPs. This effect due to the thicker solution led to better encapsulate of the drug molecules during the process of preparation of NPs [27].

In vitro CMN release

Figure 4 presents the cumulative release profiles of CMN from C-NPs. The drug release behavior of C-NPs was evaluated *in vitro* dissolution study using simulated stomach fluid at a pH of 6.8. The results indicated an initial burst release of 24% ± 2.08%, with a total release of 88.23% ± 8.91% over 24

hours. This sustained release mechanism allows for prolonged dosage release, while the initial burst release effectively reaches the desired plasma concentration. The release model that best fits the data was selected based on the correlation coefficient values from various models [28]. Initially, there was a significant difference observed, but in later, mostly *p* values were found to be significant. The C-NPs demonstrated sustained release, providing a slower and more controlled drug delivery. Maintaining a pH of 6.8 for the release of CMN was a strategic choice, as it reduces the toxicity of CMN to healthy tissues. In a related study, Mohamed *et al.* [21] found that isoniazid-based silver nanocrystals exhibited a controlled and prolonged release of the drug, lasting up to 180 minutes. The release rate was 3–4 times higher than that of free isoniazid at both pH 5.7 (weakly acidic) and pH 7.2 (neutral) conditions. The release of drugs from NP can be influenced by the ionization state of the drug and the polymer matrix. Many drugs, including CMN and isoniazid, have functional groups that can become protonated or deprotonated depending on the pH of the environment, affecting solubility and release rates. The studies have shown that CMN release from chitosan nanoparticles is significantly higher in acidic conditions (pH 5.0) compared to neutral conditions (pH 7.4). The acidic environment can enhance the solubility of CMN, leading to increased release rates [21].

The porous and biodegradable nature of chitosan NPs allows the release of encapsulated CMN in a controlled and sustained manner and the C-NP matrix might slow down the diffusion of the drug out of the particles. The hydrophilic

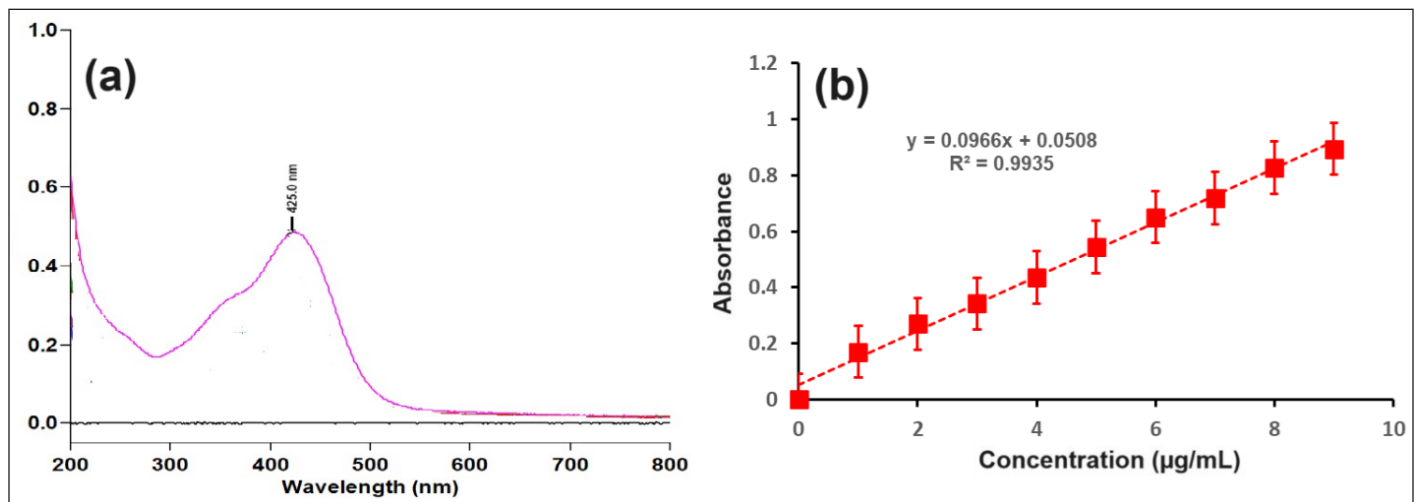


Figure 3. (a) UV Scan (at the concentration 9 µg/ml in the range of 200 to 800 nm) and (b) standard calibration curve of CMN.

Table 1. PDE (%), LC (%), drug content, and materials yield values of C-NPs.

Code	PDE (%)	LC (%)	Drug content (%)	Material loss (%)
Day 0				
B-NPs	–	–	–	2.19 ± 0.21
C-NPs	68.12 ± 4.24	86.81 ± 5.44	91.27 ± 3.34	3.71 ± 0.44
Day 15				
C-NPs	65.25 ± 6.81*	78.34 ± 8.15*	86.87 ± 6.91*	–

**p* < 0.05 indicate the significant. NPs- Blank NPs; C-SLN-Curcumin loaded NPs (mean ± SD, n = 3);

nature of chitosan helps in swelling and forming a gel-like layer around the NPs upon contact with buffer (pH 6.8) and acts as a barrier for controlling the release rate [29]. The C-NP containing chitosan degrades and releases the drug in a sustained manner with the rate of degradation can be tailored by modifying the chitosan structure.

Release kinetics

Subsequently analyzed the *in vitro* release data using the zero order, Higuchi, and Korsmeyer-Peppas models, the correlation

coefficients (R^2) were discovered to be, respectively, 0.984, 0.971, and 0.985 (Table 2). The drug release mechanism is described by the release best suited Korsmeyer-Peppas's model based on r^2 and release exponent "n" of Korsmeyer-Peppas's kinetic model. A value of "n" of 0.539 indicates that the release pertains to both the erosion and diffusion mechanisms together [30]. As the polymer erodes, drug molecules are gradually released into the surrounding medium and the rate of drug release often controlled by the rate of polymer degradation with a typical constant and sustained release profile over time. The diffusion mechanism is usually considered

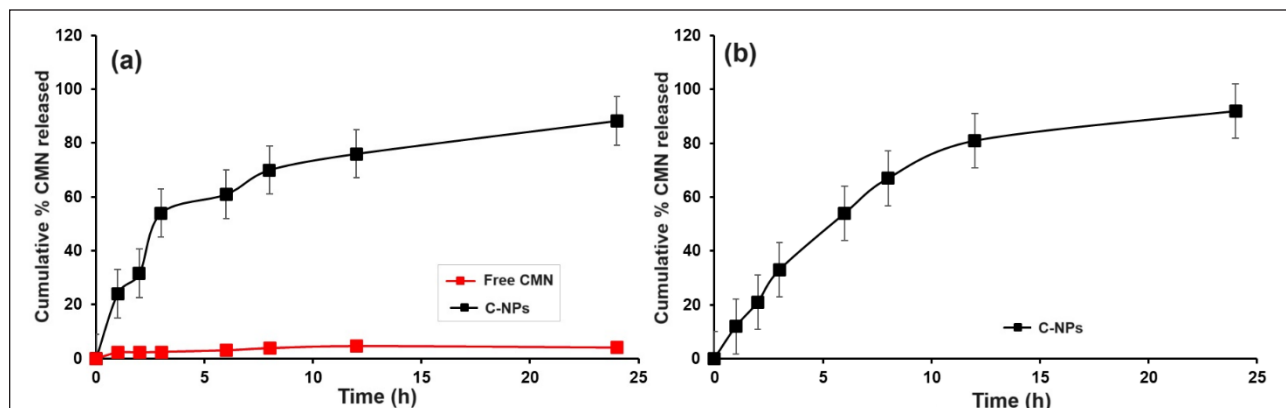


Figure 4. *In vitro* CMN release from C-NPs at (a) 24 hours (day 0) and (b) day 15 with the pH 6.8. Each value represented as mean \pm SD.

Table 2. *In vitro* CMN release kinetics of Free CMN and various C-NPs.

Codes	Correlation coefficient (r^2)					Release exponent (n)
	Zero-order	First order	Higuchi	Hixon Crowell	Korsmeyer- Peppas	
Free CMN	0.823 \pm 0.06	0.972 \pm 0.04	0.863 \pm 0.04	0.651 \pm 0.03	0.910 \pm 0.04	0.441 \pm 0.05
C-NP1	0.687 \pm 0.08	0.941 \pm 0.02	0.914 \pm 0.08	0.446 \pm 0.05	0.988 \pm 0.21	0.539 \pm 0.06

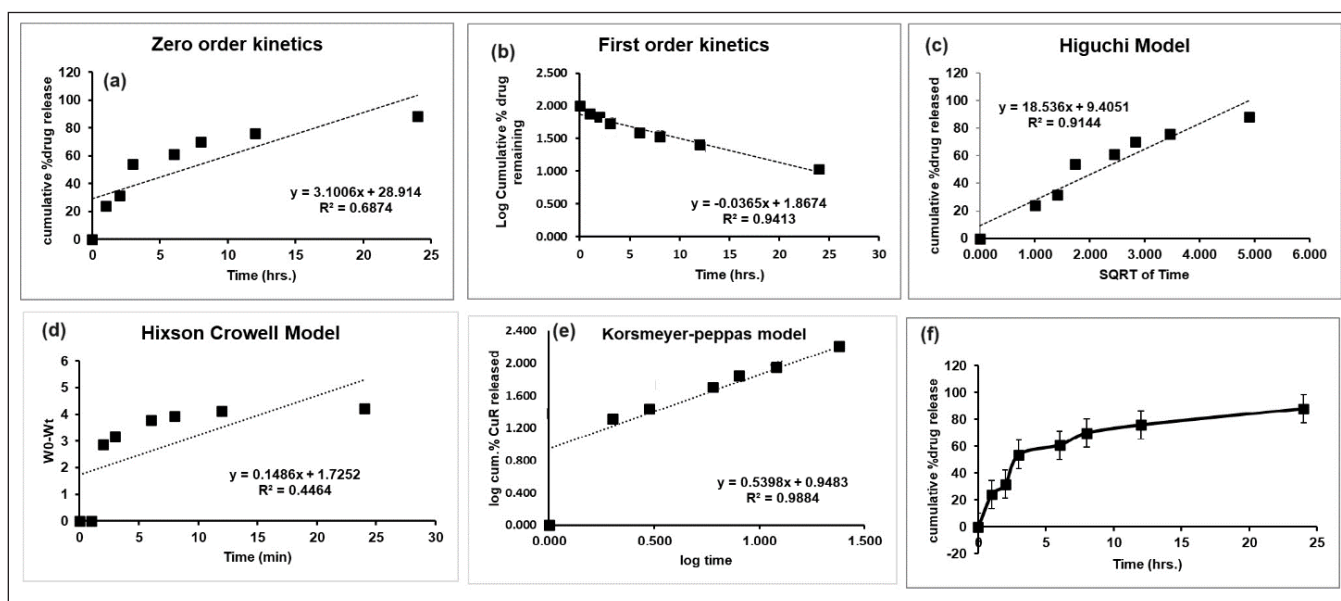


Figure 5. Mechanism of CMN release kinetics of various models such as (a) zero-order, (b) first order, (c) Higuchi model, (d) Hixson-Crowell model, (e) Korsmeyer-Peppas model, and (f) cumulative drug release from C-NP.

by an initial burst release, followed by a slower, sustained release. The release rate is influenced by factors such as the size of the drug molecules, the porosity of the polymer, and the degree of swelling of the matrix [31,32].

$n = 0.539$. This value suggests that the drug release from the dosage form is slightly deviating from Fickian diffusion (Fig. 5). It indicates that there might be some additional factors, such as polymer relaxation or swelling, influencing the release process. The value is close to 0.5 and slightly above, suggesting that the release is not purely diffusion-controlled (Non-Fickian Diffusion). These results revealed as the polymer matrix might be undergoing relaxation, which can affect the diffusional pathways [33]. Other factors, such as interactions between the drug and the matrix, might also play a role. Similar findings were found by Zhokh and Strizhak [34], who showed that the diffusion regime is considerably impacted by the pore hierarchy in the models that currently treat the pore size dependency of the diffusivity [34].

The Korsmeyer-Peppas model provides valuable insights into the mechanism of nanoparticle drug release. By understanding the release exponent, researchers can tailor the properties of NPs and polymeric matrices to achieve desired drug release profiles for various therapeutic applications.

Stability study

The prepared C-NPs were evaluated for the PDE (%), LC (%), Drug content (%), and *in vitro* drug release after 15th day. The observed results were 65.25 ± 6.81 , 78.34 ± 8.15 , 86.87 ± 6.91 , and 92.13 ± 8.27 respectively (Table 2). This result indicates the prepared NPs using chitosan as a rigid polymer protect the drug and resist or little changes from the above parameters even through quality of the product are significant ($p < 0.05$) [35]. A similar study was conducted by Walbi and co-workers [36] on curcumin-loaded lecithin/chitosan nanoparticles at $30^\circ\text{C} \pm 1^\circ\text{C}$ for 45 days with the determination of particle size, zeta potential, PDI, and %drug content and their result revealed that there were no significant changes shown, which has the good argument with the present study [36].

CONCLUSION

This study demonstrates the successful synthesis of C-NPs with favorable physicochemical properties, including high LC capacity ($86.81\% \pm 5.44\%$) and encapsulation efficiency ($68.12\% \pm 4.24\%$). FTIR analysis confirmed effective encapsulation, while *in vitro* release studies indicated a sustained release profile, aligning with the Korsmeyer-Peppas model, which suggests both erosion and diffusion mechanisms. These findings highlight the potential of C-NPs as effective carriers for CMN, enhancing its solubility, stability, and sustained release. The promising results authorize that further investigation into their *in vivo* performance and clinical applications such as cancer treatment, anti-inflammatory activity, and so on, concrete the way for improved therapeutic strategies, necessitating further *in vivo* studies to confirm efficacy and safety for clinical use.

ACKNOWLEDGMENTS

The authors would like to thank Faculty of Pharmacy & BioMedical Sciences, MAHSA University, Bandar Saujana Putra, 42610 Jenjarom, Selangor, Malaysia, for helping to carry out this FYP research project successfully.

LIST OF ABBREVIATIONS

CMN	Curcumin
C-NP	curcumin loaded chitosan nanoparticles
FT-IR	Fourier-transform infrared spectroscopy
GIT	Gastro intestinal tract
LC	Drug loading
NP	Nanoparticles
Nm	nanometer
PDE	Percentage drug entrapment

AUTHOR CONTRIBUTIONS

All authors made substantial contributions to conception and design, acquisition of data, or analysis and interpretation of data; took part in drafting the article or revising it critically for important intellectual content; agreed to submit to the current journal; gave final approval of the version to be published; and agree to be accountable for all aspects of the work. All the authors are eligible to be an author as per the International Committee of Medical Journal Editors (ICMJE) requirements/guidelines.

FINANCIAL SUPPORT DST-FIST

There is no funding to report.

CONFLICTS OF INTEREST

The authors report no financial or any other conflicts of interest in this work.

ETHICAL APPROVALS

This study does not involve experiments on animals or human subjects.

DATA AVAILABILITY

All data generated and analyzed are included in this research article.

PUBLISHER'S NOTE

All claims expressed in this article are solely those of the authors and do not necessarily represent those of the publisher, the editors and the reviewers. This journal remains neutral with regard to jurisdictional claims in published institutional affiliation.

USE OF ARTIFICIAL INTELLIGENCE (AI)-ASSISTED TECHNOLOGY

The authors declares that they have not used artificial intelligence (AI)-tools for writing and editing of the manuscript, and no images were manipulated using AI.

REFERENCES

- Altammar KA. A review on nanoparticles: characteristics, synthesis, applications, and challenges. *Front Microbiol.* 2023;14:1155622.
- Mubeen B, Ansar AN, Rasool R, Ullah I, Imam SS, Alshehri S, *et al.* Nanotechnology as a novel approach in combating microbes providing an alternative to antibiotics. *Antibiotics (Basel).* 2021;10(12):1473.
- Fathi-karkan S, Zeeshan M, Qindeel M, Malekshah RE, Rahdar A, Ferreira LF. NPs loaded with zoledronic acid as an advanced tool for cancer therapy. *J Drug Deliv Technol.* 2023;87:104805.
- Prasad S, Aggarwal BB. Turmeric, the golden spice: from traditional medicine to modern medicine. In: Benzie IFF, Wachtel-Galor S,

- editors. Herbal medicine: biomolecular and clinical aspects. 2nd ed. Boca Raton, FL: CRC Press/Taylor & Francis; 2011. Available from: <https://www.ncbi.nlm.nih.gov/books/NBK92752/>
5. Pistritto G, Trisciuglio D, Ceci C, Garufi A, D'Orazi G. Apoptosis as anticancer mechanism: function and dysfunction of its modulators and targeted therapeutic strategies. *Aging (Albany NY)*. 2016;8(4):603–19.
 6. Urošević M, Nikolić L, Gajić I, Nikolić V, Dinić A, Miljković V. Curcumin: biological activities and modern pharmaceutical forms. *Antibiotics (Basel)*. 2022;11(2):135. doi: <https://doi.org/10.3390/antibiotics11020135>
 7. Yuan S, Carter P, Bruzelius M, Vithayathil M, Kar S, Mason AM, *et al.* Effects of tumour necrosis factor on cardiovascular disease and cancer: a two-sample Mendelian randomization study. *EBioMedicine*. 2020;59:102956.
 8. Mohamed JM, Ahmad F, Kishore N, Al-Subaie AM. Soluble 1: 1 stoichiometry curcumin binary complex for potential apoptosis in human colorectal adenocarcinoma cells (SW480 and Caco-2 cells). *Res J Pharm Tech*. 2021;14(1):129–35.
 9. Shahid N, Erum A, Zaman M, Tulain UR, Shoaib QU, Malik NS, *et al.* Synthesis and evaluation of chitosan based controlled release nanoparticles for the delivery of ticagrelor. *Des Monomers Polym*. 2022;25(1):55–63. doi: <https://doi.org/10.1080/15685551.2022.2054117>
 10. Mikušová V, Mikuš P. Advances in chitosan-based nanoparticles for drug delivery. *Int J Mol Sci*. 2021;22(17):9652.
 11. Desai N, Rana D, Salave S, Gupta R, Patel P, Karunakaran B, *et al.* Chitosan: a potential biopolymer in drug delivery and biomedical applications. *Pharmaceutics*. 2023;15(4):1313.
 12. Yee Kuen C, Masarudin MJ. Chitosan nanoparticle-based system: a new insight into the promising controlled release system for lung cancer treatment. *Molecules*. 2022;27(2):473. doi: <https://doi.org/10.3390/molecules27020473>
 13. Hong L, Li W, Li Y, Yin S. Nanoparticle-based drug delivery systems targeting cancer cell surfaces. *RSC Adv*. 2023;13(31):21365–82. doi: <https://doi.org/10.1039/d3ra02969g>
 14. Karthikeyan A, Senthil N, Min T. Nanocurcumin: a promising candidate for therapeutic applications. *Front Pharmacol*. 2020;11:487. doi: <https://doi.org/10.3389/fphar.2020.00487>
 15. Moballeggh Nasery M, Abadi B, Poormoghadam D, Zarrabi A, Keyhanvar P, Khanbabaei H, *et al.* Curcumin delivery mediated by bio-based nanoparticles: a review. *Molecules*. 2020;25(3):689. doi: <https://doi.org/10.3390/molecules25030689>
 16. Wong C, Ho EA. Development of modular polymeric nanoparticles for drug delivery using amine reactive chemistry. *J Pharm Pharm Sci*. 2024;27:13148. doi: <https://doi.org/10.3389/jpps.2024.13148>
 17. Mohamed JM, Alqahtani A, Ahmad F, Krishnaraju V, Kalpana K. Stoichiometrically governed curcumin solid dispersion and its cytotoxic evaluation on colorectal adenocarcinoma cells. *Drug Des Deliv Therap*. 2020;14:4639–4658.
 18. Ahmad MZ, Rizwanullah M, Ahmad J, Alasmay MY, Akhter MH, Abdel-Wahab BA, *et al.* Progress in nanomedicine-based drug delivery in designing of chitosan nanoparticles for cancer therapy. *Int J Polym Mater Polym Biomater*. 2021;71:602–23.
 19. Hanafy AF, Abdalla AM, Guda TK, Gabr KE, Royall PG, Alqurshi A. Ocular anti-inflammatory activity of prednisolone acetate loaded chitosan-deoxycholate self-assembled nanoparticles. *Int J Nanomedicine*. 2019;14:3679–89.
 20. Prichard L, Barwick V. Preparation of calibration curves a guide to best practice. 2003. doi: <https://doi.org/10.13140/RG.2.2.36338.76488>
 21. Mohamed JMM, Alqahtani A, Kumar TVA, Fatease AA, Alqahtani T, Krishnaraju V, *et al.* Superfast synthesis of stabilized silver nanoparticles using aqueous allium sativum (garlic) extract and isoniazid hydrazide conjugates: molecular docking and *in-vitro* characterizations. *Molecules*. 2022;27(1):110.
 22. Mohamed JMM, Ahmad F, Alqahtani A, Alqahtani T, Krishnaraju V, Anusuya M. Studies on preparation and evaluation of soluble 1:1 stoichiometric curcumin complex for colorectal cancer treatment. *Trends Sci*. 2021;18(24):1403.
 23. Kakkar V, Singh S, Singla D, Kaur IP. Exploring solid lipid nanoparticles to enhance the oral bioavailability of curcumin. *Mol Nutr Food Res*. 2011;55:495–503.
 24. Seelan TV, Kumari HLJ, Kishore N, Selvamani P, Lalhlenmawia H, Thanzami K, *et al.* Exploitation of novel gum Prunus cerasoides as mucoadhesive beads for a controlled release drug delivery. *Int J Biol Macromol*. 2016;85:667–673, 156.
 25. Dai F, Zhuang Q, Huang G, Deng H, Zhang X. Infrared spectrum characteristics and quantification of OH groups in coal. *ACS Omega*. 2023;8(19):17064–76. doi: <https://doi.org/10.1021/acsomega.3c01336>
 26. Kumbhar S, Khairate R, Bhatia M, Choudhari P, Gaikwad V. Evaluation of curcumin-loaded chitosan nanoparticles for wound healing activity. *ADMET DMPK*. 2023;11(4):601–613.
 27. Amin MK, Boateng JS. Enhancing stability and mucoadhesive properties of chitosan nanoparticles by surface modification with sodium alginate and polyethylene glycol for potential oral mucosa vaccine delivery. *Mar Drugs*. 2022;20(3):156. doi: <https://doi.org/10.3390/md20030156>
 28. Mohamed JM, Alqahtani A, Ahmad F, Krishnaraju V, Kalpana K. Pectin co-functionalized dual layered solid lipid nanoparticle made by soluble curcumin for the targeted potential treatment of colorectal cancer. *Carbohydr Polym*. 2020;252:117180.
 29. Mohammed MA, Syeda JTM, Wasan KM, Wasan EK. An overview of chitosan nanoparticles and its application in non-parenteral drug delivery. *Pharmaceutics*. 2017;9(4):53.
 30. Ojsteršek T, Vrečer F, Hudovornik G. Comparative fitting of mathematical models to carvedilol release profiles obtained from hypromellose matrix tablets. *Pharmaceutics*. 2024;16:498.
 31. Visan AI, Popescu-Pelin G, Socol G. Degradation Behavior of polymers used as coating materials for drug delivery—a basic review. *Polymers (Basel)*. 2021;13(8):1272. doi: <https://doi.org/10.3390/polym13081272>
 32. Unagolla JM, Jayasuriya AC. Drug transport mechanisms and *in vitro* release kinetics of vancomycin encapsulated chitosan-alginate polyelectrolyte microparticles as a controlled drug delivery system. *Eur J Pharm Sci*. 2018;114:199–209.
 33. Fathi-Karkan S, Heidarzadeh M, Narmi MT, Mardi N, Amini H, Saghati S, *et al.* Exosome-loaded microneedle patches: promising factor delivery route. *Int J Biol Macromol*. 2023;243:125232.
 34. Zhokh A, Strizhak P. Crossover between Fickian and non-Fickian diffusion in a system with hierarchy. *Microporous Mesoporous Mater*. 2019;282:22–8.
 35. Singh G, Pai RS. Optimization (central composite design) and validation of HPLC method for investigation of emtricitabine loaded poly(lactic-co-glycolic acid) nanoparticles: *in vitro* drug release and *in vivo* pharmacokinetic studies. *Sci World J*. 2014;583090
 36. Walbi IA, Ahmad MZ, Ahmad J, Alqahtani MS, Alali AS, *et al.* Development of a curcumin-loaded lecithin/chitosan nanoparticle utilizing a box-behnken design of experiment: formulation design and influence of process parameters. *Polymers (Basel)*. 2022;14(18):3758. doi: <https://doi.org/10.3390/polym14183758>

How to cite this article:

Magdy EA, Elhassan GO, Farhana SA, Khan RA, Abdoun SA, Nachiya RAMJ, Mohamed JMM. Studies on synthesis and physiochemical evaluation of curcumin-loaded chitosan nanoparticles. *J Appl Pharm Sci*. 2025;15(08):127–134. DOI: 10.7324/JAPS.2025.220400